The Influence of Atmosphere-Ocean Interaction on MJO Development and Propagation

PI: Sue Chen
Naval Research Laboratory
Monterey, CA 93943-5502
Phone: (831) 656-4737, fax: (831) 656-4769, e-mail: sue.chen@nrlmry.navy.mil

Co-PI: James D. Doyle
Naval Research Laboratory
Monterey, CA 93943-5502
Phone: (831) 656-4716, fax: (831) 656-4769, e-mail: james.doyle@nrlmry.navy.mil

Co-PI: Paul May
Computer Sciences Corporation
Monterey, CA 93943-5502
Phone: (831) 656-4706, fax: (831) 656-4769, e-mail: paul.may@nrlmry.navy.mil

Co-PI: Jerome M. Schmidt
Naval Research Laboratory
Monterey, CA 93943-5502
Phone: (831) 656-4702, fax: (831) 656-4769, e-mail: Jerome.schmidt@nrlmry.navy.mil

Award Number: N0001413WX20817

LONG-TERM GOALS

The goals of this research are to identify the physical processes that affect the extended range prediction of the MJO and shed light on future improvements of model parameterizations and new ensemble forecast strategies that aim to increase the seasonal prediction skill of the Navy's prediction system.

OBJECTIVES

The objectives of this project are to use the fully coupled COAMPS to investigate the effect of air-ocean coupling, the prediction barrier problem near the Maritime Continent (MC), and the impact of convection permitting resolution on the MJO structure. Many coupled and uncoupled global seasonal prediction models as well as global NWP models have low skill in forecasting the MJO propagation from the Indian Ocean to the Maritime Continent. To what extent do model horizontal resolution, air-sea coupling, and parameterizations of convection contribute to this MJO propagation prediction barrier?

Report Documentation Page

Form Approved
OMB No. 0704-0188

1. REPORT DATE **30 SEP 2013**	2. REPORT TYPE	3. DATES COVERED **00-00-2013 to 00-00-2013**

4. TITLE AND SUBTITLE **The Influence of Atmosphere-Ocean Interaction on MJO Development and Propagation**	5a. CONTRACT NUMBER 5b. GRANT NUMBER 5c. PROGRAM ELEMENT NUMBER
6. AUTHOR(S)	5d. PROJECT NUMBER 5e. TASK NUMBER 5f. WORK UNIT NUMBER
7. PERFORMING ORGANIZATION NAME(S) AND ADDRESS(ES) **Naval Research Laboratory,7 Grace Hopper Avenue,Monterey,CA,93943-5502**	8. PERFORMING ORGANIZATION REPORT NUMBER
9. SPONSORING/MONITORING AGENCY NAME(S) AND ADDRESS(ES)	10. SPONSOR/MONITOR’S ACRONYM(S) 11. SPONSOR/MONITOR’S REPORT NUMBER(S)

12. DISTRIBUTION/AVAILABILITY STATEMENT
Approved for public release; distribution unlimited

13. SUPPLEMENTARY NOTES

14. ABSTRACT

15. SUBJECT TERMS

16. SECURITY CLASSIFICATION OF:			17. LIMITATION OF ABSTRACT	18. NUMBER OF PAGES	19a. NAME OF RESPONSIBLE PERSON
a. REPORT **unclassified**	b. ABSTRACT **unclassified**	c. THIS PAGE **unclassified**	**Same as Report (SAR)**	**7**	

APPROACH

The sensitivity of the MJO characteristics to air-ocean coupling processes was explored by performing various resolution (45, 15, and 5 km in the atmosphere and ocean) coupled, one-way coupled, and uncoupled 15-day forecast experiments that together form a poor-man's ensemble to investigate how the air-sea coupling, horizontal resolution, and model representation of convection impacts the MJO as it propagates through Sumatra.

The real-time European Centre for Medium-Range Weather Forecast (ECMWF) 6-hourly analysis is used in conjunction with TRMM data to provide convectively coupled wave structure. A Kelvin wave filtering of two-dimensional space and time FFT that has a cutoff wave number of 15 and time period of 2.5 days was employed to remove the high frequency diurnal signal and inertial-gravity (two-day) waves from the observed and model precipitation data. The Radon transform (Challenor et al. 2001) is used to obtain the MJO and Kelvin wave phase speed. This method is equivalent to finding the constant phase speed of the maximum energy in the wavenumber-frequency space. In addition, to compare the COAMPS ensemble forecasts with the observations, we used the MJO Limited Area Index (MLAI) technique. MLAI uses the eastward filtered model forecast of 3-hourly rain rate projected to an anomaly map to obtain the two leading EOFs. For the rain field, a 7-year 15°S-15°N averaged global TRMM 3B42 rainfall anomaly is used.

WORK COMPLETED

Two sets of 15-day poor-man's ensemble forecasts consist of a total of 17 experiments were completed. We also completed the analyses of TRMM rain and ECMWF winds for the DYNAMO MJO2.

RESULTS

We focus our initial study on the second CINDY/DYNAMO MJO (MJO2) that was initiated around 80°E on 24 Nov when the eastward propagating convective coupled Kelvin wave (CCKW) collided with a westward propagating n=1 equatorial Rossby wave. The filtered TRMM longitude and time rain analysis reveals two eastward propagating convective bands (B1 and B2) within the MJO convective envelop that encompass both the CCWK and MJO2 convection (Fig. 1). The phase speed computed by the Radon transfer for B2 gives a MJO propagation speed of 8.96 m/s. A pair of sequential CCKW ahead of the main MJO convection emerged around 1200 UTC Nov 27 west of Sumatra and Borneo (labeled CCKW1 and CCKW2 in Fig. 1). Interestingly, the Radon transform (Fig. 2) also shows two secondary energy maxima with the phase speed of 12.01 m/s and 5.5 m/s which represent a fast eastward propagation mode close to the CCKW phase speed and a slower mode that has a phase speed closer to the MJO phase speed.

We completed a set of 12-member exploratory ensemble experiments that include the initial and boundary conditions, SST, and convection uncertainties. These experiments were at 45 km horizontal resolution and were initialized at either 0000UTC or 1200UTC 20 Nov, 2011. A fixed, analysis (1-way coupled), or 2-way coupled SST were used. The ETA Kain-Fritsch (KF) or Simplified Arakawa Shubert (SAS) cumulus schemes were used in these experiments. These ensemble experiments indicate the choice of convective parameterization has more sensitivity on MJO2 propagation relative to air-sea coupling, initial condition uncertainty, and horizontal resolution. The eleven members with the KF convective scheme showed the effect of coupling is to enhance the westward propagation while

retrograde the eastward propagation. Members with a 1200UTC (5 p.m.) initialization times have stronger eastward propagation compared to members with a 0000UTC (5 a.m.) initialization times. Experiments using the SAS cumulus scheme produced a stronger MJO than KF schemes.

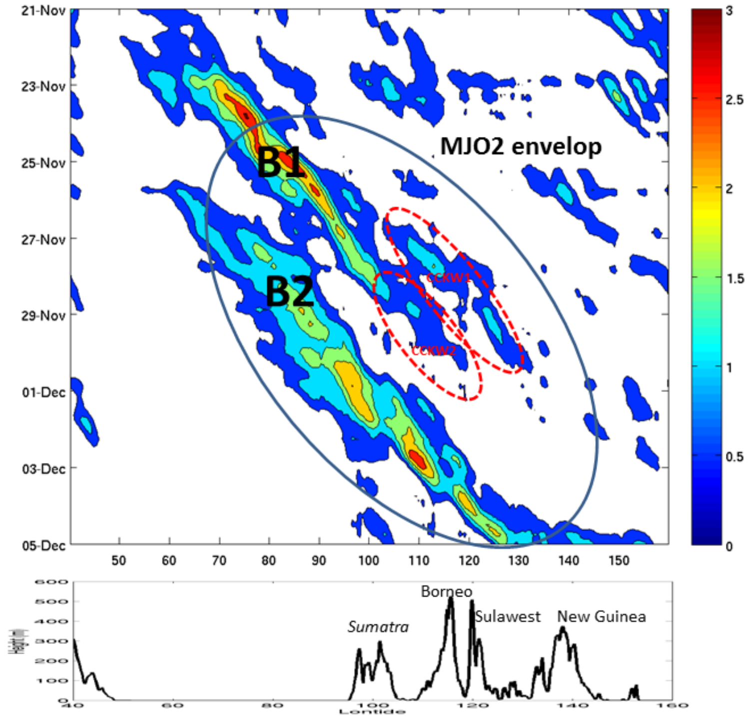

Fig. 1 Time and longitude plot of Kelvin wave filtered TRMM 3h rain averaged over 5°S to 5°N latitude band. Bottom figure is the corresponding latitude band averaged terrain height.

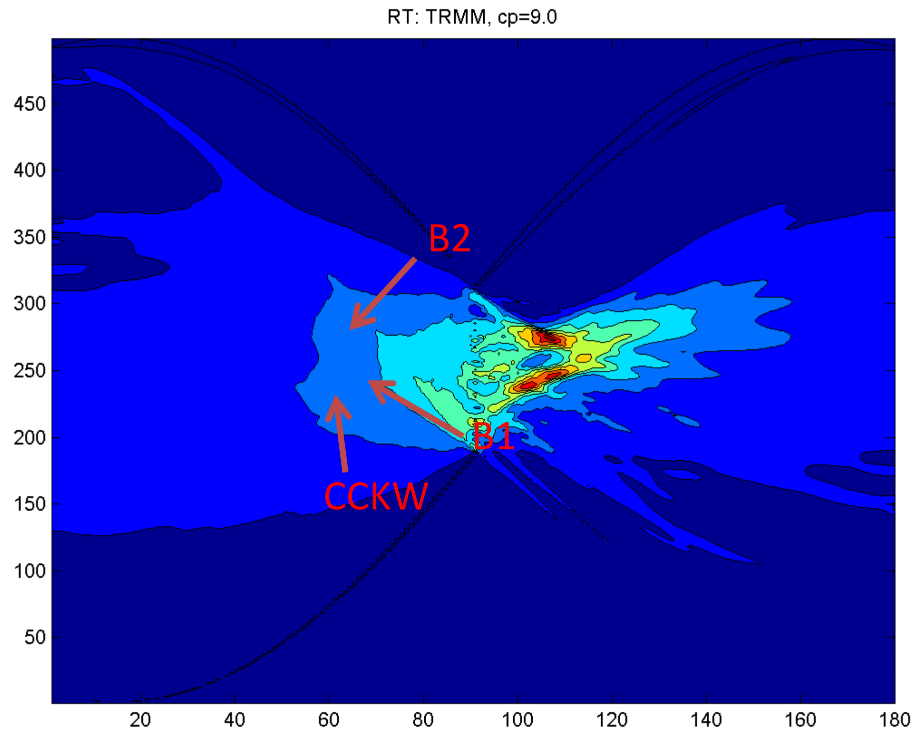

Fig. 2 The radon transform of Kelvin wave filtered TRMM precipitation from Fig. 1. The y axis is the maximum power of rain projected to the orthogonal direction of propagation and the x axis is the angle of the phase speed.

Based on the results from the exploratory ensemble, a 15km horizontal resolution 2-way coupled SAS and a 30-day 2-way coupled 45km SAS experiments was conducted. Fig.3 shows the comparison of the Hovmöller plot of the Kelvin wave filtered TRMM precipitation with these COAMPS experiments. The SAS15 has the phase speed of 7.9 m/s which is closer to TRMM. However, it had the CCKW damped out faster than TRMM before reaching Sumatra. The phase speed of 45km coupled (uncoupled) SAS are much slower than the 15km SAS which is 3.03 (4.62) m/s. Uncoupled experiments using 15km COAMPS KF produced a fast CCKW but a much weaker B2 convective band compared to TRMM. The ETA KF has the weakest eastward propagating MJO envelop. Encouraging results were obtained from a 30-day 45km SAS forecast from 5 Nov to 5 Dec. The model initial time is 18 days before the MJO2 initiation at 80°E on 24 Nov. Compared to the 3-day lead time 15-day SAS 45km experiment and TRMM, both COAMPS 45km 18-day and 3-day lead time forecasts have the MJO2 double eastward propagating bands with westerly wind burst to the west of convection. However, the SAS 45km 30-day forecast had too much precipitation that covers a larger area compared to TRMM. The 45km SAS 30-day forecast MJO2 initiation time is also few days earlier than TRMM. Overall the 20- and 15-day domain averaged 45 km SAS precipitation pattern is similar to TRMM but both predicted stronger tropical depression in Bay of Bengal.

This feature agrees with the analysis of eastward component of MJO Limited Area (MLAI) index. The COAMPS 15km SAS shows there is a time delay of COAMPS EOF1 and EOF2 compare to TRMM (not shown) but the maximum values of EOF1 and EOF2 are comparable with TRMM. The EOF1 represents enhanced convection variance in central IO. While EOF2 gives the variance of the

convection approaching MC. The combination of TRMM EOF1 and EOF2 explain about 16% of total precipitation variability (Flatau et al. 2013).

To investigate the sensitivity of convective process on MJO propagation, we conducted several idealized COAMPS tests on the convective closures. These results showed considerable sensitivity to the parameterized entrainment/precipitation rate. In addition, a simple 1-D model is used to illustrate that the resolvable-scale precipitation is sensitive to the model update of the mass-weighted mean terminal velocity at the beginning of each small time-step within the time-splitting loop used in the sedimentation calculation.

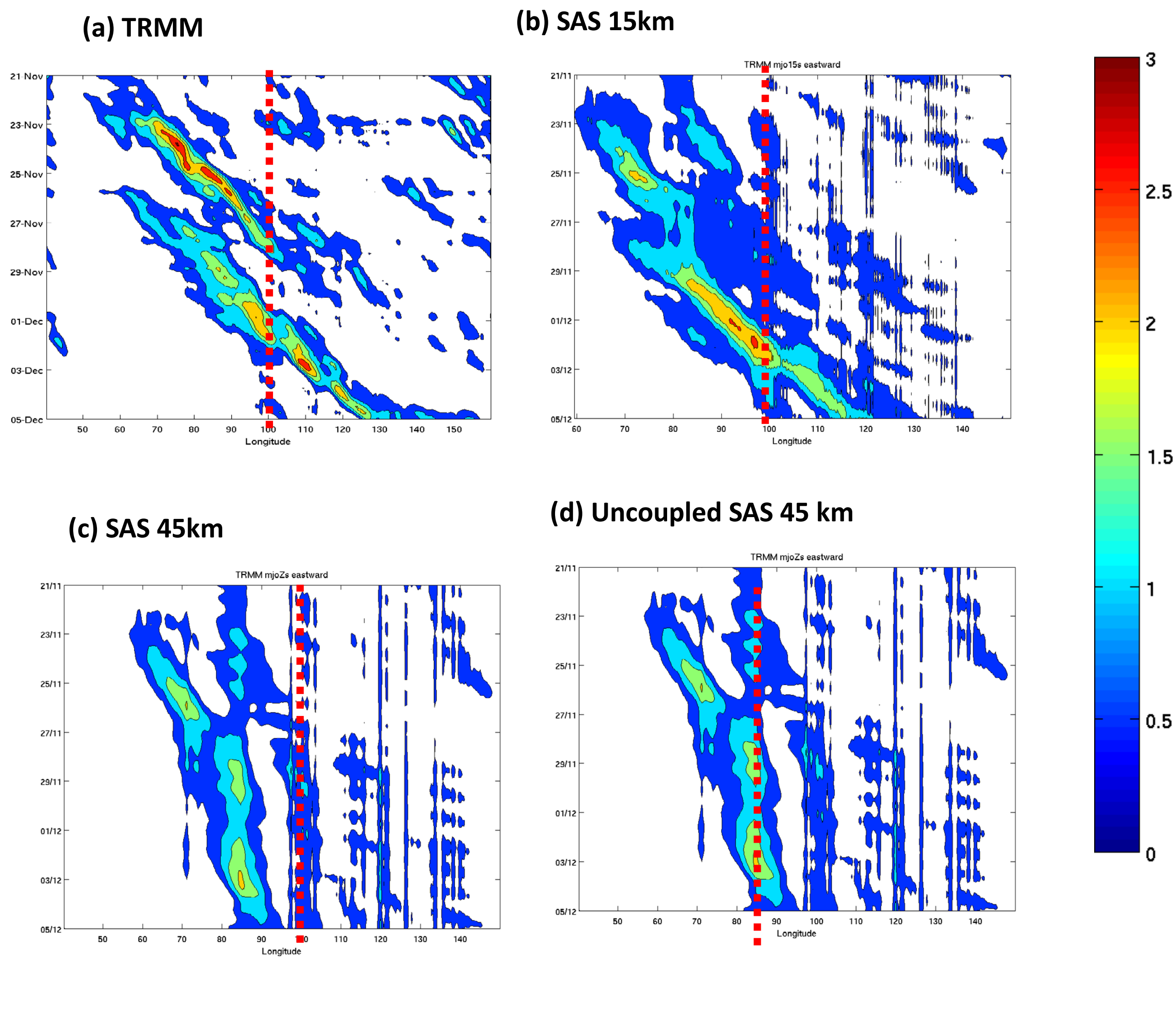

Fig. 3 Time-longitude plots of Kelvin wave filtered rain for (a) TRMM, (b) coupled COAMPS 15km SAS, (c) coupled COAMPS 45km SAS, and (d) uncoupled COAMPS 45km SAS. The red dashed line indicates the position of Sumatra around 100 °E.

A synthesis of TRMM rainfall and ECMWF analysis shows that a preconditioning of the CCKW that formed a pair of counter-rotating gyre west of Sumatra enhances both the kinetic and moist static energy of subsequent MJO2 main convective envelop (B2). The gyre allows for MJO2 to overcome the blocking of the Barisan mountain range on Sumatra. The large-scale flow pattern at the time when MJO2 was propagating from Indian Ocean to MC is shown by the real-time ECMWF 850 hPa zonal wind speed (m/s) analysis from 28 Nov to 1 December, 2011. The environmental flow was comprised of a tropical depression north of 10°N in the Arabian Sea, a large area of westerly wind burst west of MJO2 on the equator, two CCKW 10-20 degree east of MJO2, and a cyclonic gyre induced by CCKW2 south of equator on 0000UTC, 28 Nov (Fig. 4a) which later turned into a pair of counter-rotating westward propagating Rossby wave by 1 Dec (Fig. 4b). This feature is similar to the oceanic Kelvin wave that was observed to reflect at the eastern boundary and return as poleward propagating coastal Kelvin waves and westward propagating equatorial Rossby waves. The change of flow field by CCKW ahead of the MJO is analyzed by examining ocean area inside the stagnation zone. We averaged the ECMWF fields in two 3° (93°E-96°E) x12° (6°S to 6°N) and 3° (96°E-99°E) x6° (0 to 6°N) longitude and latitudes boxes. The results reveal during the transition time from CCKW to MJO between 28 Nov and 3 Dec, the column integrated total kinetic energy from 1000 to 20 hPa within the box doubled from 1000 m^2/s^2 to 2100 m^2/s^2. This increase of kinetic energy was contributed to by the increased westerly wind between 900-500 hPa and northerly wind between 700-400 hPa. The ejection of the gyre kinetic energy transformed the MJO flow field from zonal to wave-like circulations that eventually caused a shift of the MJO to flow southward cross the lower barrier in southern Sumatra.

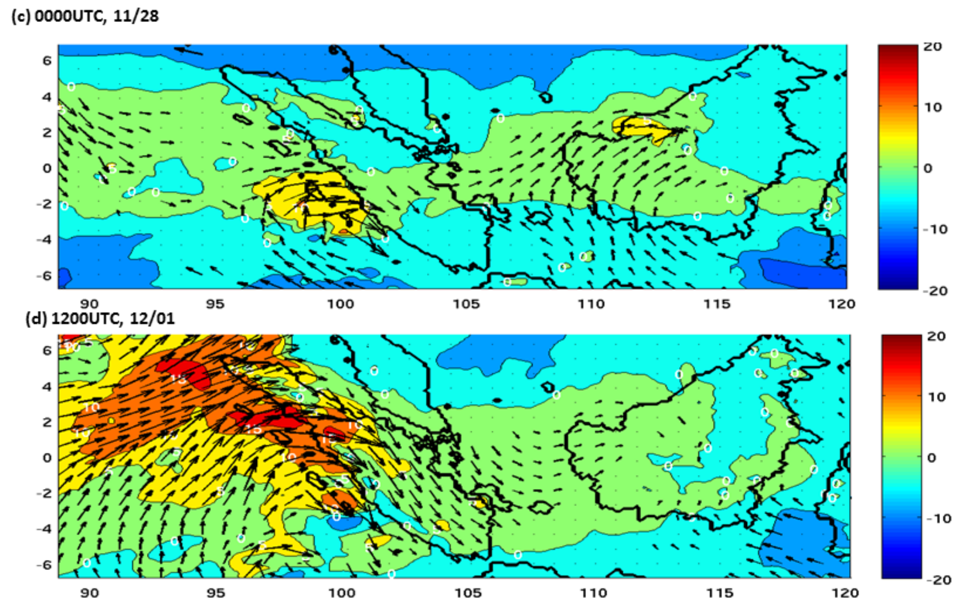

Fig. 4 (a) ECMWF 850 hPa zonal wind speed (m/s) on 0000UTC 28 Nov. (b) As in (a) but for 200UTC 1 Dec. The small wind vectors for u and v wind speed < 2 m/s are masked out to enhance the wind feature.

Comparison of COAMPS best member, the15km SAS, 850 hPa zonal wind with the ECMWF analysis indicates that COAMPS failed to produce the CCKW ahead of main MJO convective band B2 and the CCKW southern gyre seen in ECMWF analysis. COAMPS 850 hPa wind showed more southerly instead of westerly ahead of main MJO super cloud clusters which leads to increased blocking period of the MJO2 kinetic energy west of Sumatra that is about a day longer. Our results suggest the

prediction of the initiation and magnitude of MJO2 convection is critical in maintaining an energetic CCKW and subsequent MJO2 propagation is dependent on the prediction of CCKW.

REFERENCES

Challenor, P. G., Cipollini, P., & Cromwell, D. (2001), Use of the 3D Radon transform to examine the properties of oceanic Rossby waves. J. of Atmos. and Oceanic Tech., 18(9), 1558-1566.

Flatau, M., S. Chen, T. Shinoda, T. G. Jensen, D. Baranowski, A. Vintzeilaos , T. Nasuno , 2013: Evaluating MJO precipitation in limited area models. MWR, submitted

RELATED PROJECTS

This project is closely related to a number of ONR programs on “Coupled MJO”, “Impact of resolution on extended-range multi-scale simulations”, and “Physics parameterization for seasonal prediction”.

PUBLICATIONS

Chen, S., P. W. May, M. Flatau, J. M. Schmidt, and J. Doyle, 2013: Preconditioning of convective coupled Kelvin waves on the CINDY/DYNAMO November MJO propagation, to be submitted to JGR letter.

Schmidt, M. J., 2013: A subtle error in sedimentation calculations used in standard bulk cloud microphysics schemes, to be submitted to MWR.